End States and Subgap Structure in Proximity-Coupled Chains of Magnetic Adatoms

Michael Ruby,[1] Falko Pientka,[2] Yang Peng,[2] Felix von Oppen,[2] Benjamin W. Heinrich,[1] and Katharina J. Franke[1]
[1]Fachbereich Physik, Freie Universität Berlin, 14195 Berlin, Germany
[2]Dahlem Center for Complex Quantum Systems and Fachbereich Physik, Freie Universität Berlin, 14195 Berlin, Germany
(Received 21 July 2015; published 4 November 2015)

A recent experiment [Nadj-Perge *et al.*, Science 346, 602 (2014)] provides evidence for Majorana zero modes in iron (Fe) chains on the superconducting Pb(110) surface. Here, we study this system by scanning tunneling microscopy using superconducting tips. This high-resolution technique resolves a rich subgap structure, including zero-energy excitations in some chains. We compare the symmetry properties of the data under voltage reversal against theoretical expectations and provide evidence that the putative Majorana signature overlaps with a previously unresolved low-energy resonance. Interpreting the data within a Majorana framework suggests that the topological gap is smaller than previously extracted from experiment. Aided by model calculations, we also analyze higher-energy features of the subgap spectrum and their relation to high-bias peaks which we associate with the Fe d bands.

DOI: 10.1103/PhysRevLett.115.197204 PACS numbers: 73.63.Nm, 74.20.-z, 75.70.Tj, 75.75.-c

Building on advances in nanofabrication [1], engineering topological phases by proximity in superconducting hybrid structures has come within reach of current experiments. A major motivation for realizing such phases is their non-Abelian Majorana quasiparticles [2–4], and their subsequent applications. The underlying topological superconducting phases can be realized in one-dimensional (1D) helical liquids contacted by conventional s-wave superconductors [5–9]. Among the most promising platforms studied in experiments are semiconductor nanowires [10–14], edges of two-dimensional topological insulators [15,16], and chains of magnetic adatoms [17,18]. While the proximity coupling to a superconductor is needed to induce a gap protecting the topological phase, it also has more subtle consequences. Magnetic interactions mediated by the superconductor can stabilize magnetic order in the 1D system [19–22]. Conversely, the spin structure may affect the superconductor. This is particularly apparent for adatom chains, where a band of subgap Shiba states [23–26] may strongly modify the low-energy properties of the system [8,27–31] and possibly induce trivial zero-energy features at the chain end [32]. At strong coupling, the 1D states bleed substantially into the superconductor, reducing the effective coherence length at low energies [33].

Nadj-Perge *et al.* [17] recently provided intriguing evidence for Majorana states in Fe chains on Pb(110). Here, we present data on the same system employing scanning tunneling microscopy (STM) and scanning tunneling spectroscopy (STS) with superconducting tips (see also Ref. [17]). We show that the use of superconducting tips not only provides enhanced resolution of the subgap structure but also allows for additional consistency checks on the interpretation of the data in terms of Majorana quasiparticles. Our observations indicate that the subgap spectrum comprises a flat Shiba band and strongly dispersing Fe states. An interpretation in terms of Majorana states suggests that the induced gap is smaller than the value previously extracted from experiment.

We carried out the experiments in a SPECS JT-STM at a temperature of 1.1 K. Cycles of sputtering and annealing of a Pb(110) single crystal ($T_c = 7.2$ K) resulted in an atomically flat and clean surface. We employed Pb-covered superconducting tips (see Ref. [34] for the preparation procedure), which provide a resolution beyond the Fermi-Dirac limit [35–37] (in our measurements: $\simeq 70\ \mu$V). Fe chains were prepared by e-beam evaporation from an iron rod (99.99% purity) onto the clean surface at room temperature, similar to Ref. [17]. Without further annealing, we obtained chain lengths of up to $\simeq 10$ nm (measured between the chain end and the intervening Fe cluster). Single adatoms and dimers were prepared by e-beam evaporation onto the cold sample in the STM ($T < 10$ K) with a density of ≈ 350 adatoms per 100×100 nm^2. The differential conductance dI/dV as a function of sample bias was recorded using standard lock-in technique at 912 Hz (subgap spectra: bias modulation $V_{\mathrm{mod}} = 15\ \mu V_{\mathrm{rms}}$, set point $V = 5$ mV, $I = 250$ pA; large-scale spectra: $V_{\mathrm{mod}} = 2\ \mathrm{mV_{rms}}$, $V = 2$ V, $I = 850$ pA).

STS with a superconducting tip measures a convolution of the density of states of tip and sample as long as the tunneling rate is slower than the quasiparticle relaxation of the subgap states [38]. This is the case for all measurements presented in this Letter. As the tunneling electrons leave behind an unpaired electron in the tip, sample resonances are shifted by $\pm\Delta_{\mathrm{tip}}$, the superconducting gap parameter of the tip. The coherence peaks of the superconductor appear at $eV = \pm(\Delta_{\mathrm{tip}} + \Delta_{\mathrm{sample}})$, while a subgap state of energy ε yields a resonance peak at $eV = \pm(\Delta_{\mathrm{tip}} + \varepsilon)$. Accordingly, zero-energy Majorana states are signaled by resonances at $eV = \pm\Delta_{\mathrm{tip}}$ [17]. At finite temperatures, quasiparticles can

be thermally excited to the unoccupied subgap states. These excited quasiparticles contribute to tunneling and yield additional, "thermal" resonances that appear at $\pm(\Delta_{tip} - \varepsilon)$ [34,38]. At our experimental temperature, this effect is limited to small energies ε.

Figure 1 shows subgap dI/dV spectra, recorded at the termination of six independent Fe chains. Figures 1(a)–(d) display chains terminated by a small cluster, visible as a protrusion in the STM images. The chains in Figs. 1(a) and 1(d) exhibit a clear zero-energy signature at a bias of $+\Delta_{tip}$, which has been interpreted as a fingerprint of a Majorana bound state [17] (for the determination of the value of Δ_{tip}, see the Supplemental Material [39]). The zero-energy feature is accompanied by two resonances at higher energies. In contrast, the chains in Figs. 1(b) and 1(c) do not exhibit a clear peak at $+\Delta_{tip}$, but they exhibit a low-energy resonance at a bias of around 1.47 and 1.52 mV, respectively. Figures 1(e) and 1(f) show data for chains without a protrusion at their ends. These appear rarely, and we can only provide data with reduced resolution ($\simeq$330 μV) due to inferior tip preparation. These chains also lack an unambiguous signature of a zero-energy resonance, perhaps masked by the larger resonance, which contributes considerable spectral intensity at Δ_{tip}. However, the presence of a Majorana state only depends on the topological phase in the chain and should not be affected by structural details of the chain end, as long as the termination has a (trivial) energy gap.

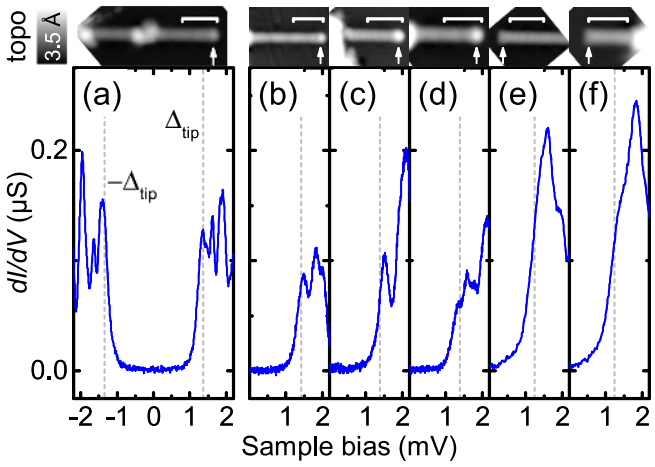

FIG. 1 (color online). dI/dV spectra recorded at the end of six different chains (small arrows mark the position on the chain). Chains in (a)–(d) are terminated by a small cluster; in (e),(f) they have a sharp cutoff. The energy resolution in (e),(f) is reduced (width of BCS resonance: $\simeq$330 μV) due to nonbulklike superconductivity of the tip. Δ_{tip} in meV: (a) 1.36; (b) 1.42; (c),(d) 1.38; (e),(f) 1.24. Chain lengths measured between the chain end and the cluster onset in nm: (a) 13.9, (b) 9.5, (c) 6.2, (d) 6.0, (e) 7.7, (f) 4.0. Scale bars correspond to 4 nm. For the full spectra of (b)–(f), see the Supplemental Material [39].

Figure 1(a) shows that the peaks at opposite biases $\pm\Delta_{tip}$ differ substantially in intensity. The same is observed in all other chains [39]. This is in contrast to expectations for Majorana peaks, which should be symmetric because a Majorana state has identical electron and hole wave functions [40]. This indicates that these peaks originate, at least partially, from trivial subgap states near zero energy. For a more detailed analysis, we focus on the chains shown in Figs. 1(a) and 1(b).

It is interesting to contrast the spectra of chains with those of individual Fe adatoms and dimers. Figure 2(a) shows the dI/dV signal of two species of single adatoms with different apparent heights. For both types, we observe a single, shallow Shiba state at $\varepsilon \simeq 1.1$ meV (type 1) and $\varepsilon \simeq 1.2$ meV (type 2), respectively. In contrast, the dimer shown in Fig. 2(b) exhibits a richer subgap structure with a series of resonances with energies as low as $\simeq$150 μeV. We find that the subgap spectrum varies in detail between different dimers, depending on interatomic distance, angle, and adsorption site [39]. This demonstrates strong coupling

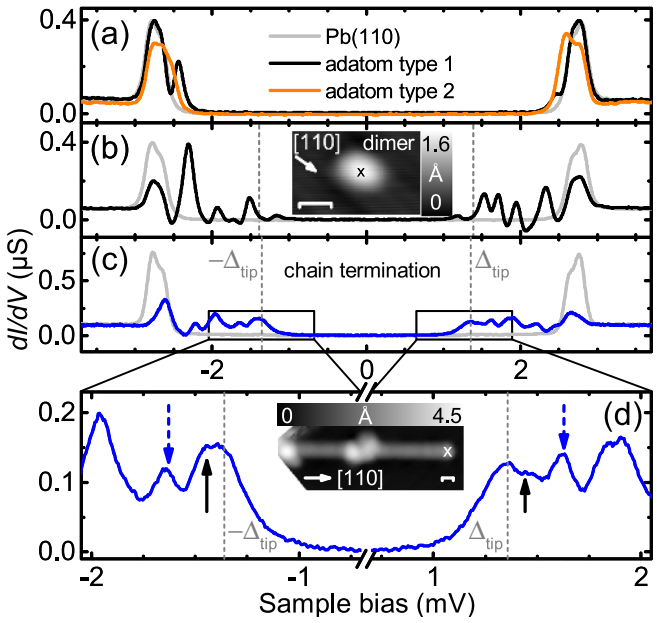

FIG. 2 (color online). dI/dV spectra of different Fe entities on Pb(110). (a) Two types of single adatoms: both spectra exhibit a single Shiba resonance close to the gap edge. The adatoms differ in apparent height by $\simeq$20 pm at 50 mV, 50 pA. (b) Fe dimer: a variety of Shiba states with the lowest energy resonance at $\varepsilon \simeq 150$ μeV is observed. $\Delta_{tip} = 1.39$ meV. (c) Chain end (the blue line) as in Fig. 1(a), and bare Pb(110) (the gray line) for comparison. (d) Zoom on (c): a manifold of Shiba resonances is resolved. A peak at $+\Delta_{tip}$ may be the fingerprint of a Majorana bound state. Low-energy states lie at $\varepsilon \simeq 80$ μeV (the black solid arrow) and $\varepsilon \simeq 270$ μeV (the blue dashed arrow). At 1.1 K, low intensity thermal resonances are expected at $(\pm\Delta_{tip} - \varepsilon)$ [38]. Albeit not resolvable, they contribute to the tail in intensity at biases between $\pm\Delta_{tip}$. Scale bars in the topography insets correspond to 1 nm.

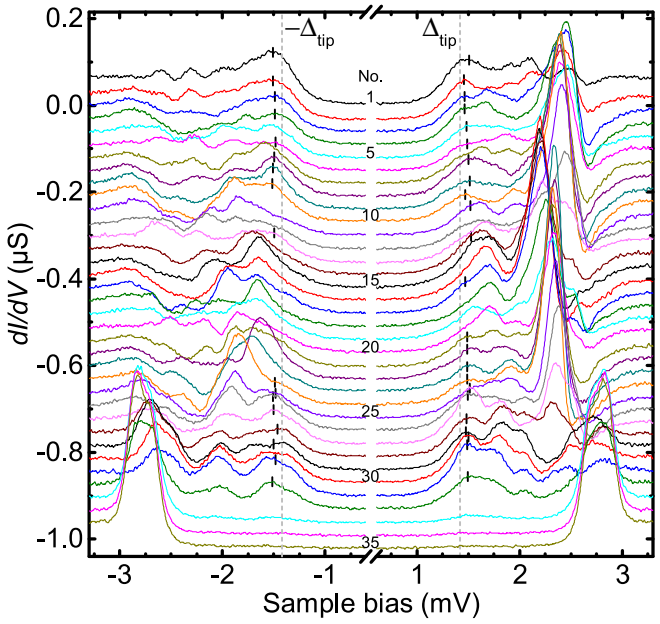

FIG. 3 (color online). Spatially resolved dI/dV spectra along the chain in Fig. 1(b), going from the onset of the Fe cluster (No. 1) to the bare surface (No. 35). At the chain end [No. 29, same as in Fig. 1(b) and Fig. S2(b)], a zero-energy resonance at $-\Delta_{tip}$, and at the Fe cluster (No. 1), a resonance at $+\Delta_{tip}$ are visible as local maxima. At the opposite bias, a shoulder is observed. The lowest nonzero energy resonance is found at $\varepsilon \simeq 80$ μeV in No. 29 and is modulated along the chain. As a guide for the eye, local maxima or shoulders with energies $0 < \varepsilon < 100$ μeV are marked by ticks. The high intensity peaks at positive bias shift along the chain with ε ranging from 700 to 1000 μeV. Offset for clarity: −30 nS/spectrum. Distance between spectra: 0.33 nm. $\Delta_{tip} = 1.42$ meV.

of Shiba states which can ultimately lead to the formation of Shiba bands in adatom chains.

Figure 2(c) provides the data of Fig. 1(a) over a wider voltage range, with a zoom in on the voltage range near Δ_{tip} shown in Fig. 2(d). In addition to the peak at $+\Delta_{tip}$ and a faint shoulder at $-\Delta_{tip}$, there is a nearby subgap resonance at $\varepsilon \simeq 80$ μeV (the black solid arrows). These combine into a plateaulike structure near and just above $\pm\Delta_{tip}$. The data are also consistent with corresponding thermal resonances at $\pm(\Delta_{tip} - 80$ μeV). The superposition with a low-energy subgap resonance may explain the asymmetric peaks in Fig. 1(a). While a Majorana peak must be symmetric, conventional subgap resonances can be asymmetric, reflecting the asymmetry between the electron and hole wave functions.

Further subgap peaks occur at higher energies, the next higher one at $\varepsilon \simeq 270$ μeV [the blue dashed arrows in Fig. 2(d)]. Similar peaks were identified in Ref. [17] as the coherence peaks of the induced topological gap (estimated at 200–300 μeV). In view of the lower-energy peaks, this interpretation seems implausible for our chains. Instead, a Majorana-based interpretation would suggest that the lowest nonzero energy peak originates from the topological gap or is shifted above the topological gap by size quantization. This suggests that the topological gap is comparable to or smaller than $\simeq$80 μeV.

While the Majorana states should be localized at the chain end, the topological gap is a property of the bulk spectrum and should be observable throughout the entire chain. In Fig. 3, we present spatially resolved dI/dV spectra of the same chain as in Fig. 1(b) [and Fig. S2(b)]. Spectra at the end of the chain, e.g., Nos. 1 and 29, exhibit a peak or shoulder at $\pm\Delta_{tip}$. The asymmetry may again be due to the overlap with nearby resonances with energies below 100 μeV. The latter resonances are observable throughout the chain, but they vary in intensity and/or energy (marked in Fig. 3). This is in contrast to the zero-energy resonances, which only exist at the ends of the chain.

The most likely scenario for topological superconductivity in adatom chains is that an odd number of spin-polarized d bands cross the Pb Fermi energy

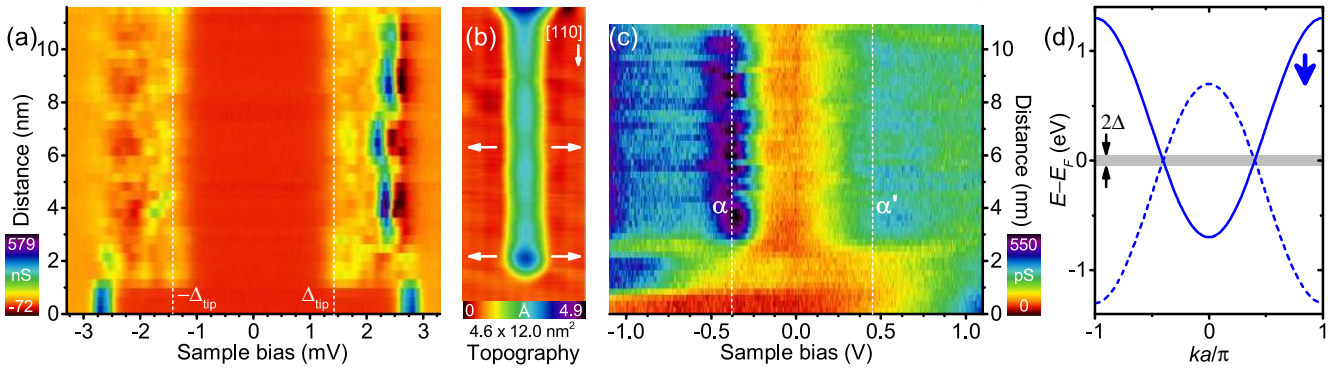

FIG. 4 (color online). False-color plot of the dI/dV spectra of (a) the subgap (the same spectra as in Fig. 3) and (c) the d-band structure, aligned with the topography in (b). The subgap structure (a) exhibits variations of the Shiba peak energies and intensities, as well as modulations of the low-energy resonance at $\varepsilon \simeq 80$ μeV along the chain. A zero-energy resonance is found at both chain terminations. Resonances linked to the d-band structure (c) vary around −380 mV (α), and 450 mV (α') along the chain. (d) Sketch of a spin-polarized d band (the full line) and its hole complement (the dashed line) crossing the Fermi level of the superconductor.

[9,17,33], as illustrated in Fig. 4(d). Spin-orbit coupling in the substrate enables proximity-induced p-wave pairing even for ferromagnetic chains. The subgap bands combine the rapidly dispersing d bands, yielding gapped V-shaped structures and weakly dispersing Shiba-like states near $k = 0$ and $k = \pi/a$, where the d bands are far from the Fermi energy. The resulting subgap band is illustrated in Fig. 5(c) for a chain of spin-1/2 Anderson impurities on a BCS superconductor, assuming that the spin-up band is fully occupied and the spin-down band crosses the Pb Fermi energy. We now explore these relations between subgap excitations and high-energy band structure.

The weakly dispersing Shiba states contribute van Hove–like subgap resonances at nonzero energies. Indeed, in addition to the resonance at $\varepsilon \simeq 270$ μeV already mentioned above, many of the spectra exhibit a strong subgap resonance at a bias of $\simeq$2.3 mV. The false-color plot in Fig. 4(a) (the same dI/dV spectra as in Fig. 3) reveals that its intensity oscillates with a period of $\simeq$2 nm and shifts slightly to lower energy in the center of the chain. The lower-energy resonances near $\pm\Delta_{\mathrm{tip}}$ do not show such a clear periodicity. Interestingly, the periodic variations appear correlated with the topography of the chain, as shown next to the false-color plot in Fig. 4(b). The apparent height and width of the chain show variations with a similar period of $\simeq$2 nm, in agreement with Ref. [17].

Moreover, the band edges of the Fe d bands contribute van Hove peaks in STS. In Fig. 4(c), we provide a false-color plot of dI/dV spectra along the chain in a larger bias range between $\pm$1.1 V. In the interior of the chain, we observe two prominent features: a narrow resonance α at around -380 mV and a broader resonance α' at around 450 mV. Similar resonances are present for all chains shown in Fig. 1, and they are in agreement with Ref. [17]. These resonances decrease in intensity and finally disappear at the end of the chain or close to the Fe cluster, respectively (see additional traces in Ref. [39]). We

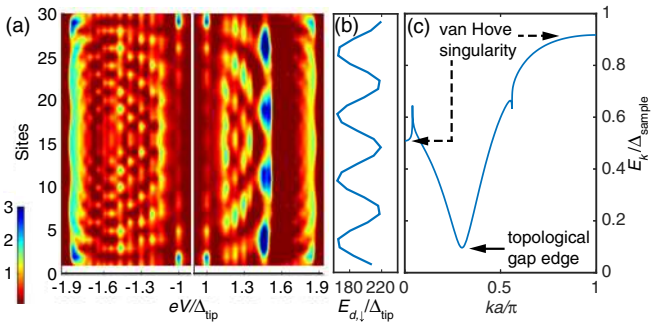

FIG. 5 (color online). Numerical results for a chain of 30 sites. (a) Color plot of the differential conductance along the chain at subgap energies for a superconducting tip. (b) Spatially varying on-site energies of impurity levels. (c) Bulk subgap band structure of an impurity chain on the surface of an s-wave superconductor. We used $\Delta_{\mathrm{sample}}/\Delta_{\mathrm{tip}} = 0.958$. See Ref. [39] for other parameters.

interpret these resonances as the van Hove singularities of the d bands. The simultaneous disappearance of α and α' suggests that these are the upper and lower edges of the same band crossing the Fermi level. Interestingly, resonance α shifts with the above observed periodicity of about 2 nm [39].

To understand how the spatial variations in the d bands affect the peaks in the subgap spectra, we have performed model calculations for a chain of Anderson impurities coupled to an s-wave superconductor with spin-orbit coupling (see Refs. [33] and [39]). We model the modulations by a potential which varies along the chain and reflects the local environment of the adatoms [see Fig. 5(b)]. We choose parameters such that one band crosses the Fermi level with band edges corresponding to α and α' and assume strong adatom-substrate coupling. Following Ref. [33], we calculate the subgap local density of states from a mean-field treatment of the impurity chain (see Ref. [39]) and the differential conductance. As temperature exceeds the typical energy separation between subgap levels, we assume efficient quasiparticle relaxation, which results in dominant single-particle tunneling. The experimental resolution is modeled by broadening of the tip density of states. Note that these conditions preclude the observation of a quantized Majorana peak height [40].

Figure 5(a) shows the subgap differential conductance of a finite chain, including the spatially varying potential. The numerical results are consistent with key features of the experimental data. (i) The Majorana bound state has a short decay length of a few lattice sites as a consequence of the strong chain-substrate coupling [33]. (ii) Prominent peaks at $eV = \pm 1.5\Delta_{\mathrm{tip}}$ and $\pm 1.9\Delta_{\mathrm{tip}}$ signal the van Hove singularities of the Shiba band. Their intensity modulations are correlated with the potential landscape of the impurity atoms. Here, the effect of the corrugation is most visible because the Shiba energy explicitly depends on the energy of the impurity level. (iii) The induced gap varies along the chain on atomic scales but is uncorrelated with the potential landscape. Indeed, at strong coupling the induced gap only depends on the substrate gap and the spin-orbit interaction and is insensitive to details of the impurities. The fluctuations reflect finite-size quantization which is most visible at low energies due to the low density of states in the V-shaped dip of the band structure [Fig. 5(c)].

Motivated by Ref. [17], we investigated the subgap spectra and the possible Majorana signatures of Fe chains on a superconducting Pb(110) substrate by scanning tunneling spectroscopy. Using superconducting tips, a Majorana state is expected to appear as a pair of resonances at $\pm\Delta_{\mathrm{tip}}$ with symmetric intensities. We associate the absence of this symmetry in the data with a nearby low-energy subgap resonance at 80 μeV. Within a Majorana framework, it is natural to interpret this additional resonance as the coherence peak of the induced topological gap, which would then be smaller than previously measured. We

show by model calculations that such an interpretation is, in principle, consistent with our observations. However, a conclusive confirmation of Majorana end states in adatom chains would be greatly facilitated by experiments at considerably lower temperatures. Using superconducting tips at temperatures well below the induced gap might even provide access to the elusive conductance quantization of Majorana states [40].

We acknowledge financial support by the Deutsche Forschungsgemeinschaft through the collaborative research center SFB 658 and Grant No. FR2726/4 (K. F.), as well as research priority programs SPP 1285 and SPP 1666 (F. v. O.), and also by a Consolidator Grant from the European Research Council "NanoSpin" (K. F.) and by the Helmholtz Virtual Institute "New States of Matter and Their Excitations" (F. v. O.).

[1] S. De Franceschi, L. Kouwenhoven, C. Schönenberger, and W. Wernsdorfer, Nat. Nanotechnol. **5**, 703 (2010).
[2] J. Alicea, Rep. Prog. Phys. **75**, 076501 (2012).
[3] C. W. J. Beenakker, Annu. Rev. Condens. Matter Phys. **4**, 113 (2013).
[4] S. R. Elliott and M. Franz, Rev. Mod. Phys. **87**, 137 (2015).
[5] L. Fu and C. L. Kane, Phys. Rev. B **79**, 161408(R) (2009).
[6] R. M. Lutchyn, J. D. Sau, and S. Das Sarma, Phys. Rev. Lett. **105**, 077001 (2010).
[7] Y. Oreg, G. Refael, and F. von Oppen, Phys. Rev. Lett. **105**, 177002 (2010).
[8] S. Nadj-Perge, I. K. Drozdov, B. A. Bernevig, and A. Yazdani, Phys. Rev. B **88**, 020407(R) (2013).
[9] J. Li, H. Chen, I. K. Drozdov, A. Yazdani, B. A. Bernevig, and A. H. MacDonald, Phys. Rev. B **90**, 235433 (2014).
[10] V. Mourik, K. Zuo, S. M. Frolov, S. R. Plissard, E. P. A. M. Bakkers, and L. P. Kouwenhoven, Science **336**, 1003 (2012).
[11] A. Das, Y. Ronen, Y. Most, Y. Oreg, M. Heiblum, and H. Shtrikman, Nat. Phys. **8**, 887 (2012).
[12] H. O. H. Churchill, V. Fatemi, K. Grove-Rasmussen, M. T. Deng, P. Caroff, H. Q. Xu, and C. M. Marcus, Phys. Rev. B **87**, 241401(R) (2013).
[13] M. T. Deng, C. L. Yu, G. Y. Huang, M. Larsson, P. Caroff, and H. Q. Xu, Nano Lett. **12**, 6414 (2012).
[14] A. D. K. Finck, D. J. Van Harlingen, P. K. Mohseni, K. Jung, and X. Li, Phys. Rev. Lett. **110**, 126406 (2013).
[15] S. Hart, H. Ren, T. Wagner, P. Leubner, M. Mühlbauer, C. Brüne, H. Buhmann, L. W. Molenkamp, and A. Yacoby, Nat. Phys. **10**, 638 (2014).
[16] V. S. Pribiag, A. J. A. Beukman, F. Qu, M. C. Cassidy, C. Charpentier, W. Wegscheider, and L. P. Kouwenhoven, Nat. Nanotechnol. **10**, 593 (2015).
[17] S. Nadj-Perge, I. K. Drozdov, J. Li, H. Chen, S. Jeon, J. Seo, A. H. MacDonald, B. A. Bernevig, and A. Yazdani, Science **346**, 602 (2014).
[18] R. Pawlak, M. Kisiel, J. Klinovaja, T. Meier, S. Kawai, T. Glatzel, D. Loss, and E. Meyer, arXiv:1505.06078.
[19] B. Braunecker and P. Simon, Phys. Rev. Lett. **111**, 147202 (2013).
[20] J. Klinovaja, P. Stano, A. Yazdani, and D. Loss, Phys. Rev. Lett. **111**, 186805 (2013).
[21] M. M. Vazifeh and M. Franz, Phys. Rev. Lett. **111**, 206802 (2013).
[22] Y. Kim, M. Cheng, B. Bauer, R. M. Lutchyn, and S. Das Sarma, Phys. Rev. B **90**, 060401(R) (2014).
[23] L. Yu, Acta Phys. Sin. **21**, 75 (1965).
[24] H. Shiba, Prog. Theor. Phys. **40**, 435 (1968).
[25] A. I. Rusinov, Zh. Eksp. Teor. Fiz., Pis'ma Red. **9**, 146 (1968) [JETP Lett. **9**, 85 (1969)].
[26] A. V. Balatsky, I. Vekhter, and J.-X. Zhu, Rev. Mod. Phys. **78**, 373 (2006).
[27] F. Pientka, L. I. Glazman, and F. von Oppen, Phys. Rev. B **88**, 155420 (2013).
[28] S. Nakosai, Y. Tanaka, and N. Nagaosa, Phys. Rev. B **88**, 180503(R) (2013).
[29] K. Pöyhönen, A. Westström, J. Röntynen, and T. Ojanen, Phys. Rev. B **89**, 115109 (2014).
[30] A. Heimes, P. Kotetes, and G. Schön, Phys. Rev. B **90**, 060507(R) (2014).
[31] P. M. R. Brydon, S. Das Sarma, H. Y. Hui, and J. D. Sau, Phys. Rev. B **91**, 064505 (2015).
[32] J. D. Sau and P. M. R. Brydon, Phys. Rev. Lett. **115**, 127003 (2015).
[33] Y. Peng, F. Pientka, L. I. Glazman, and F. von Oppen, Phys. Rev. Lett. **114**, 106801 (2015).
[34] K. J. Franke, G. Schulze, and J. I. Pascual, Science **332**, 940 (2011).
[35] S.-H. Ji, T. Zhang, Y.-S. Fu, X. Chen, X.-C. Ma, J. Li, W.-H. Duan, J.-F. Jia, and Q.-K. Xue, Phys. Rev. Lett. **100**, 226801 (2008).
[36] B. W. Heinrich, L. Braun, J. I. Pascual, and K. J. Franke, Nat. Phys. **9**, 765 (2013).
[37] M. Ruby, B. W. Heinrich, J. I. Pascual, and K. J. Franke, Phys. Rev. Lett. **114**, 157001 (2015).
[38] M. Ruby, F. Pientka, Y. Peng, F. von Oppen, B. W. Heinrich, and K. J. Franke, Phys. Rev. Lett. **115**, 087001 (2015).
[39] See Supplemental Material at http://link.aps.org/supplemental/10.1103/PhysRevLett.115.197204 for additional data on Fe dimers and Fe chains, the method to determine the tip gap, and the theoretical model.
[40] Y. Peng, F. Pientka, Y. Vinkler-Aviv, L. I. Glazman, and F. von Oppen, arXiv:1506.06763.